Biogeosciences Discuss., 10, 10459–10489, 2013
www.biogeosciences-discuss.net/10/10459/2013/
doi:10.5194/bgd-10-10459-2013

Biogeosciences Discussions
Open Access

Spatio-temporal patterns of C : N : P ratios in the northern Benguela upwelling regime

A. Flohr[1], A. K. van der Plas[2], K.-C. Emeis[3,4], V. Mohrholz[5], and T. Rixen[1,4]

[1]Leibniz Centre for Tropical Marine Ecology (ZMT), Fahrenheitstraße 6, 28359 Bremen, Germany
[2]National Marine Information and Research Centre, Ministry of Fisheries & Marine Resources, P.O. Box 912 Swakopmund, Namibia
[3]Helmholtz-Centre for Materials and Coastal Research Geesthacht, Max-Planck-Straße 1, 21502 Geesthacht, Germany
[4]Institute for Biogeochemistry and Marine Chemistry, University of Hamburg, Bundesstraße 55, 20146 Hamburg, Germany
[5]Leibniz-Institute for Baltic Sea Research, Seestraße 15, 18119 Rostock, Germany

Received: 3 June 2013 – Accepted: 9 June 2013 – Published: 27 June 2013

Correspondence to: A. Flohr (anita.flohr@zmt-bremen.de)

Published by Copernicus Publications on behalf of the European Geosciences Union.

Abstract

Dissolved carbon to nutrient ratios in the oceans' interior are remarkably consistent with the classical $C : N : P : O_2$ Redfield ratio of $106 : 16 : 1 : 138$ reflecting the mean composition of organic matter photosynthesized in the sunlit surface ocean. Deviations from the Redfield ratio indicate changes in the functioning of the biological carbon pump, which is driven and limited by the availability of nutrients. The northern Benguela coastal upwelling system (NBUS) is known for losses of fixed nitrogen ($N = NO_3^-$, NO_2^- and NH_4^+) and the accumulation of phosphate (P) in sub- and anoxic bottom waters and sediments of the Namibian shelf. To study the impact on the regional carbon cycle and consequences for the nutrient export from the BUS into the oligotrophic subtropical gyre of the South Atlantic Ocean we measured dissolved inorganic carbon (C_T), oxygen (O_2), and nutrient concentrations as well as the total alkalinity (A_T) in February 2011. Our results indicate that over the Namibian shelf the $C : N : P : O_2$ ratio decreases to $106 : 16 : 1.6 : 138$ because of phosphate efflux from sediments. N reduction further increase $C : N$ and reduce $N : P$ ratios in those regions where O_2 concentrations in bottom waters are $< 20\,\mu mol\,kg^{-1}$. However, off the shelf along the continental margin the mean $C : N : P : O_2$ ratio is again close to the Redfield stoichiometry. Comparing the situation of 2011 with nutrient concentration data measured during 2 cruises in 2008 and 2009 implies that the amount of excess P that is created in the bottom waters on the shelf and its export into the subtropical gyre after upwelling varies through time. The magnitude of excess P formation and export is governed by inputs of excess N along with the South Atlantic Central Water (SACW) flowing into the NBUS from the north as a poleward compensation current. Since excess N is produced by the remineralization of N-enriched biomass built up by N_2-fixing organisms, factors controlling N_2 fixation north of the BUS need to be addressed in future studies to better understand the NBUS' role as P source and N sink in the coupled $C : N : P$ cycles.

BGD
10, 10459–10489, 2013

1 Introduction

The biological carbon pump is the term used for the production of organic carbon from dissolved carbon dioxide (CO_2) in the surface mixed layer of the ocean and its transport into the large CO_2 reservoir of the ocean beneath the mixed layer. It is both driven and limited by the availability of macronutrients, such as carbon (C), fixed nitrogen (N), and phosphate (P), as well as micronutrients such as iron (Watson et al., 2000; Behrenfeld et al., 2006b). Macronutrients are required in specific stoichiometric ratios for the photosynthetic production of organic matter traditionally termed as Redfield ratio of C : N : P = 106 : 16 : 1 (Redfield et al., 1963). Changes of the Redfield ratio could strongly influence the marine productivity and the oceans' ability to sequester CO_2 from the atmosphere (McElroy, 1983; Heinze et al., 1991; Falkowski, 1997).

On a global scale the C : N : P ratios of dissolved carbon and nutrients in the ocean are remarkably consistent with the traditional Redfield ratio of C : N : P = 106 : 16 : 1 for the photosynthetic production of organic matter (Redfield et al., 1963; Takahashi et al., 1985; Anderson and Sarmiento, 1994). Nevertheless on a more regional scale a pronounced variability of C : N : P ratios exists. The C : N : P ratio of phytoplankton shows sensitivity to nutrient availability, growth rate, taxonomy and ambient CO_2 concentrations (Arrigo, 2005; Riebesell et al., 2007).

Eastern boundary upwelling systems (EBUS) are regions of high CO_2 concentrations (Boehme et al., 1998; Torres et al., 1999) and intense biological production and export of carbon (Carr, 2002). They as well play an important role in supplying nutrients to the surface mixed layer of adjacent oligotrophic subtropical gyres where nutrient supply is limited by stable thermal stratification (Behrenfeld et al., 2006a). The Benguela upwelling system (BUS) is a coastal upwelling system known for non-standard nutrient (N : P) ratios in upwelling waters (Tyrrell and Lucas, 2002) caused by N reduction (anammox and/or denitrification) and P release from sediments in low O_2 environments (Kuypers et al., 2005; Nagel et al., 2013). The C : N : P remineralization ratios in the

BGD
10, 10459–10489, 2013

subsurface waters are poorly constrained but are crucial in order to characterize the cycling of C in the BUS.

We analyzed nutrient (NO_3^-, NO_2^-, P) and dissolved O_2 data in conjunction with data on dissolved inorganic carbon (C_T) and alkalinity (A_T) raised during an expedition in 2011, and complemented these with nutrient data from 2 other expeditions staged in 2008 and 2009. Our objectives were to identify the spatial variability of the C : N : P : O_2 mineralization ratios of the northern BUS (NBUS), to study the spatial and temporal variability of biogeochemical conditions influencing the N losses, and associated consequences for the nutrient export from the eutrophic upwelling system into the oligotrophic subtropical gyre.

2 Material and methods

2.1 Study area

The BUS spans along the south western coast of Africa, covering the western South African and Namibian coastline roughly from Cape Agulhas (~ 34° S) to the Angola Benguela Frontal Zone (ABFZ) (Hutchings et al., 2009) (Fig. 1a). At the ABFZ, which is centred between 14° S and 16° S (Meeuwis and Lutjeharms, 1990) but is highly dynamic in terms of shape and location, the cold Benguela current system converges with warm tropical waters of the surface Angola Current (AC). To the south, the system is bordered by the Agulhas Current that reverses and partly converges with the South Atlantic water resulting in the formation of eddies (Agulhas Rings, AR) and filaments (Hall and Lutjeharms, 2011).

Along the coast of SW Africa, the interaction of southerly trade winds with coastal topography forces upwelling, which is strongest at 3 distinct upwelling cells (Shillington et al., 2006; Hutchings et al., 2009). The Lüderitz upwelling cell (~ 26° S) accounts for roughly 50 % of physical upwelling and separates the upwelling region into a northern and a southern subsystem (Shannon, 1985; Duncombe Rae, 2005). In the southern

BGD
10, 10459–10489, 2013

region (south of 26° S) the trade winds are seasonal and upwelling has maxima during austral spring and summer. The northern region (from 26° S to the ABFZ) is characterized by perennial alongshore winds and upwelling along the coast (Shannon, 1985).

The Lüderitz cell also marks the boundary of two intermediate water regimes that cause distinct differences in biogeochemical properties of upwelling waters. Upwelling in the southern BUS entrains Eastern South Atlantic Water (ESACW) into the offshore Ekman drift at the surface (Duncombe Rae, 2005; Mohrholz et al., 2007). The ESACW is an intermediate water mass formed at the Brazil–Falkland confluence off South America (Gordon, 1981; Stramma and England, 1999) and flows along with the southern branch of the Subtropical Gyre and the Benguela Current northwards into the NBUS (Gordon, 1981; Sprintall and Tomczak, 1993; Poole and Tomczak, 1999). Here, the ESACW mixes with an Angola Gyre subtype of the South Atlantic Central Water (SACW). The SACW originates in the subtropical Angola Gyre and forms a poleward undercurrent flowing along the continental margin and the Namibian shelf break (Duncombe Rae, 2005; Mohrholz et al., 2007). The SACW is originally a branch of ESACW that penetrated further northward into the equatorial system of intermediate water masses. It is older than the ESACW and thus enriched in CO_2 and nutrients, and depleted in O_2. Increased inflow of SACW into the NBUS preconditions the development of an oxygen minimum zone (OMZ) and anoxic events over the Namibian shelf and upper slope (Weeks et al., 2002; Monteiro et al., 2006; Mohrholz et al., 2007).

On the shelf at low O_2 concentrations ($< 20\,\mu M\,O_2$) NO_x is reduced by denitrification and/or anammox (Lam and Kuypers, 2010; Kalvelage et al., 2011). The loss of fixed N to anammox within the OMZ on the shelf has been estimated to $\sim 1.4\,Tg\,N\,a^{-1}$ (Kuypers et al., 2005) and the loss to denitrification to $\sim 2.5\,Tg\,N\,a^{-1}$ (Nagel et al., 2013). However, N loss exceeds estimates on N_2 fixation (Sohm et al., 2011) suggesting that the BUS acts as net sink for fixed N. Furthermore, the BUS shelf is a region of modern phosphorite deposition (Glenn et al., 1994; Föllmi, 1996) associated with a massive organic rich diatomaceous mud belt that roughly follows the Namibian coast between 50 and 200 m water depth and covers an area of $\sim 18\,000\,km^2$ (Bremner,

BGD
10, 10459–10489, 2013

1980; Bremner and Willis, 1993; Emeis et al., 2004). The mud belt surface is settled by consortia of large sulphur bacteria (including *Thiomargarita namibiens*) that release phosphate (PO_4^{3-}) into the anoxic pore water (Nathan et al., 1993; Schulz and Schulz, 2005; Goldhammer et al., 2010) and enrich pore waters with concentrations of up to ~ 1000 µM PO_4^{3-} (van der Plas et al., 2007).

2.2 Water sampling and analysis

Nutrient samples were collected during three cruises in austral summer and early autumn (Fig. 1b): MSM07/2b-3 (RV *Maria S. Merian*, 9 March–17 April 2008), Afr258 (RV *Africana*, 1–17 December 2009) and the MSM17/3 (RV *Maria S. Merian*, 31 January–8 March 2011). Sampled transects perpendicular to the coast stretched from the shelf, over the continental slope and into the open ocean. At least five stations per transect were sampled off Kunene (17.25° S), Rocky Point (19.00° S), Terrace Bay (20.00° S), Toscanini (20.80° S) and Walvis Bay (23.00° S). Of these transects Kunene, Rocky Point and Walvis Bay where sampled during all of the three cruises. Samples were collected by CTD casts using a rosette system equipped with 10 L Niskin bottles. The analyzed parameters presented in this study comprise dissolved inorganic carbon (C_T), total alkalinity (A_T) and dissolved nutrients (NO_x = nitrate (NO_3^-) + nitrite (NO_2^-) and phosphate (PO_4^{3-})).

2.2.1 C_T and A_T

The C_T and A_T samples were taken during the MSM17/3 cruise. Transects off Kunene (17.25° S), Rocky Point (19.00° S), Terrace Bay (20.00° S), Toscanini (20.80° S) and Walvis Bay (23.00° S) were sampled. For C_T and A_T analysis the samples were filled in 250 mL borosilicate bottles using silicone tubes (Tygon). The bottles were rinsed twice and filled from the bottom to avoid bubbles. Periodically duplicate samples were taken. The samples were fixed with mercuric chloride solution (250 µL of a 35 g L^{-1} $HgCl_2$) directly after collection and analyzed on board using the VINDTA 3C system (Marianda,

BGD
10, 10459–10489, 2013

Kiel, Germany). The A_T was determined on the basis of the open cell principle. The samples were titrated with a fixed volume of hydrochloric acid by equal increments of HCl (0.1 N HCl). For the determination of C_T, the CO_2 was extracted out of acidified water samples and quantified by the coulorimetric method with a precision of 0.1 %. Certified Reference Material (CRM, batch #101 and #104, provided by A. Dickson (Scripps Institution of Oceanography, La Jolla, CA, USA)) was used to calibrate the VINDTA 3C system. The C_T and A_T measurements of duplicate samples agreed to $\pm 2\,\mu mol\,kg^{-1}$. In the following A_T is reported as the salinity corrected value ($A_T = A_{Tmeas} \times 35/S_{meas}$).

2.2.2 Dissolved nutrients

The nutrient samples were filtered through disposable syringe filters (0.45 µm) immediately after sampling, filled in pre-rinsed 50 mL PE bottles and frozen (−20 °C). Samples collected during the MSM07/2b-3 cruise were measured on board, whereas samples taken during Afr258 and MSM17/3 cruises were analyzed in the shore-based laboratory subsequently to the expedition. Dissolved nutrients were measured by a continuous flow injection system (Skalar SAN plus System) according to methods described by Grasshoff et al. (1999). The detection limits were: $NO_x = 0.08\,\mu M$ and $PO_4^3 = 0.07\,\mu M$ according to DIN 32645. Ammonium (NH_4^+) concentrations were usually $< 2.5\,\mu mol\,kg^{-1}$ and are not discussed in this paper.

2.3 Characterization of SACW and ESACW

The potential temperature (T_{pot}) and salinity characteristics were used to differentiate between SACW and ESACW contributions. Their definitions were adopted from Mohrholz et al. (2007), who identified an Angola Gyre subtype of SACW. The ESACW and SACW are defined by a line in T_{pot} – Salinity (S) space that can be described by

BGD
10, 10459–10489, 2013

the following equations:

$$T_{\text{pot ESACW}} = 9.4454 \cdot S_{\text{ESACW}} - 319.03 \quad (1)$$

$$T_{\text{pot SACW}} = 8.5607 \cdot S_{\text{SACW}} - 289.08 \quad (2)$$

The above equations were transformed to calculate the respective proportions of SACW and ESACW:

$$S_{\text{SACW}} = (T_{\text{pot}} + 289.08)/8.5607 \quad (3)$$

$$S_{\text{ESACW}} = (T_{\text{pot}} + 319.03)/9.4454 \quad (4)$$

$$S_{\text{measured}} = a \cdot S_{\text{SACW}} + b \cdot S_{\text{ESACW}}, \text{ whereby } a + b = 1 \quad (5)$$

The relative contribution of SACW and ESACW are reported in percentage [%]. Data derived from water depths < 100 m were excluded from this mixing analysis due to the non-conservative behaviour of T_{pot} and S at shallower water depths.

2.4 Anomalies of N : P stoichiometry

To calculate the deviation from the classical Redfield ratio (N : P = 16 : 1) (Redfield et al., 1963) we used the tracer N* (Gruber and Sarmiento, 1997):

$$\text{N}^* = \left([\text{NO}_3^-] - 16 \cdot [\text{PO}_4^{3-}] + 2.9\right) \cdot 0.87 \quad (6)$$

Positive and negative N* imply a relative excess or deficit of nitrate and nitrite (N) relative to phosphate (P), respectively, whereas N* = 0 represents the global mean value that has an N deficit of $-2.9\,\mu\text{mol}\,\text{kg}^{-1}$ at $0\,\mu\text{mol}\,\text{kg}^{-1}$ P (or a P excess of $0.18\,\mu\text{mol}\,\text{kg}^{-1}$). For better comparability with literature we use the concept of Deutsch et al. (2007) to quantify the P anomaly (P*) from Redfield:

$$\text{P}^* = [\text{PO}_4^{3-}] - [\text{NO}_3^-]/16 \quad (7)$$

BGD
10, 10459–10489, 2013

3 Results and discussion

It has been shown that on a global scale the distribution of N : P is characterized by a relative deficit of N towards P. The intercept of global N : P nutrient data indicate a P excess of $\sim 0.18\,\mu mol\,kg^{-1}$ in the global surface ocean (Gruber and Sarmiento, 1997) and the mean slope is with N : P = 14–15 : 1 below the classical Redfield correlation of N : P = 16 : 1 (Redfield et al., 1963) due to a net loss of fixed N that, as mentioned before, occurs e.g. within the OMZ on the Namibian shelf (Kuypers et al., 2005; Nagel et al., 2013). In the following the C : N : P remineralization patterns observed in 2011 are discussed with regard to their spatial variability and are complemented by results on the temporal variability of N : P anomalies recorded in 2008 and 2009.

3.1 C : N : P : AOU stoichiometry

The NO_x and PO_4^{3-} concentrations from the NBUS scattered to both sides of the reference Redfield slope and characterize the NBUS as a system that produces both positive and negative deviations from Redfield expressed in positive and negative N^* anomalies (Fig. 2). Major negative anomalies were apparent at shelf sites. Tyrrell and Lucas (2002) attributed low N : P (LNP) data (N : P < 3 and $PO_4^{3-} > 1.5\,\mu mol\,kg^{-1}$) in waters of the BUS to nutrient trapping and denitrification that leads to a relative accumulation of P. Figure 3 illustrates the relationships between apparent oxygen utilization (AOU) calculated from O_2 concentrations, NO_x ($NO_3^- + NO_2^-$), PO_4^{3-} and C_T of the water samples in 2011 (MSM17/3). The observed average C_T : AOU ratio of 0.76 ($r^2 = 0.89$) is close to that expected from a mineralization C:O_2 ratio of 106 : −138 (Fig. 3a). Exclusion of the $O_2 < 20\,\mu mol\,kg^{-1}$ data gave no mentionable differences between the shelf (C_T : AOU = 0.77, $r^2 = 0.88$) and offshore sites (C_T : AOU = 0.75, $r^2 = 0.89$). The scattering of data in Fig. 3a is likely due to the fact that the shelf system is not truly closed and that O_2 is introduced into the subsurface water masses on the shelf through mixing (Ito et al., 2004). The increase of C_T at AOU > $250\,\mu mol\,kg^{-1}$ corresponding to

BGD
10, 10459–10489, 2013

$O_2 < 20\,\mu mol\,kg^{-1}$ implies C_T input from anerobic respiration, such as denitrification and is evident from decreasing NO_x associated with increasing C_T concentrations at $O_2 < 20\,\mu mol\,kg^{-1}$ (Fig. 3b). At higher O_2 the overall average $C_T : NO_x = 6.1$ ($r^2 = 0.86$) is similar to the Redfield ratio of 6.6 with slightly lower values in the open ocean (5.5, $r^2 = 0.89$) than on the shelf (6.8, $r^2 = 0.86$). The slope of the $A_T : C_T \sim -0.15$ (Fig. 4) observed in the paired data agrees with the expected effect of aerobic organic matter remineralization ($A_T : C_T = -16 : 106$) ratio due to the release of CO_2 and NO_3^- (Broecker and Peng, 1982) and imply that carbonate dissolution hardly affected the C_T and the A_T concentrations. At O_2 concentrations $< 20\,\mu mol\,kg^{-1}$, both anammox and denitrification increase A_T through the consumption of NO_x. However, a decrease in C_T indicating a dominance of anammox over heterotrophic denitrification is not visible in our data (Fig. 3b) likely due to the low C : N stoichiometry of anammox (C : N $\sim -0.07 : -1.3$) compared to that of denitrification (C : N $\sim 106 : -104$) (Koeve and Kähler, 2010). A loss of NO_x by $20\,\mu mol\,kg^{-1}$ would result in a C_T decrease of $-1\,\mu mol\,kg^{-1}$ due to anammox and a C_T increase of $+21\,\mu mol\,kg^{-1}$ during denitrification.

A source for PO_4^{3-} besides mineralization of organic matter in the water column is suggested by the spread of $C_T : PO_4^{3-}$ data in Fig. 3c. Open ocean sites had an average $C_T : PO_4^{3-}$ ratio of 101 : 1 that is similar to the global mean C : P ratio of 106 : 1 (Redfield et al., 1963; Anderson and Sarmiento, 1994). The $C_T : PO_4^{3-}$ correlation of the shelf data splits in 2 groups. One group revealed a slope of the regression line of $\sim 98 : 1$ ($r^2 = 0.82$) which is similar to those seen in the offshore samples. The remaining samples suggest a much lower average $C_T : PO_4^{3-}$ ratio of ~ 65 ($r^2 = 0.84$) and are related to the mud belt region off Walvis Bay. Even lower C : P ratios of 48–33 were measured in pore waters near the sediment water interface within the mud belt (Goldhammer et al., 2011). Because PO_4^{3-} concentrations higher than expected from mineralization of organic matter occurred exclusively at shelf sites the low $C_T : PO_4^{3-}$ imply an impact of pore water P-effluxes from anoxic sediments mediated by consortia

BGD
10, 10459–10489, 2013

of sulphur bacteria (Schulz and Schulz, 2005). This in line with previous hypotheses that the stoichiometric N deficit in waters over the Namibian shelf is, next to the impact of NO_x reduction, in part caused by P fluxes across the sediment water interface (Bailey and Chapman, 1991; Nagel et al., 2013). The impact of NO_x loss and benthic fluxes of PO_4^{3-} at low O_2 concentrations is underscored by the decoupling of PO_4^{3-} and NO_x maxima along the Namibian shelf and slope (Fig. 5; exemplary for the MSM17/3 cruise in February 2011). The mid-water OMZ off Kunene (17.25° S) disappeared towards the south and instead the OMZ was restricted to the shelf off 23° S. Pore water effluxes at low O_2 concentrations shifted as well, so that $PO_{4\,max}^{3-}$ occurred off the shelf in the north ($PO_{4\,max}^{3-}$ = 2.5 µmol kg^{-1}) and within the OMZ on the shelf ($PO_{4\,max}^{3-}$ = 4.8 µmol kg^{-1}) in the south (off 23° S). Due to N losses at low O_2 concentrations, the NO_x maxima were observed outside the OMZ and decreased from 45 µmol kg^{-1} (17.25° S) to 35 µmol kg^{-1} (23° S). Although the N loss likely contributes to the overall NO_x decrease, it also reflects the gradual increase of ESACW fraction towards the south. This water mass is characterized by lower nutrient concentrations than SACW (Poole and Tomczak, 1999; Mohrholz et al., 2007).

Concluding, C : N : P : O_2 ratios at offshore sites are 101 : 16 : 1 : 138 and are stoichiometrically close to Redfield ratios, whereas PO_4^{3-} input lowers the C : N : P : O_2 ratio to 106 : 16 : 1.6 : 138 over the shelf off Walvis Bay. Only in regions with O_2 concentrations < 20 µmol kg^{-1}, denitrification increases C : N and denitrification and anammox further lower N : P ratios.

3.2 Spatial and temporal variability

Inter-annual differences in upwelling conditions during austral summer expeditions were well reflected in the distribution of sea surface temperatures (SST). The SST patterns, measured continuously by thermo-salinographs at 5 m water depth, indicate that upwelling was most intense in December 2009 (Afr258) (Fig. 6), when minimum SST (15 °C) occurred along the entire coast and temperatures < 20 °C were measured

BGD
10, 10459–10489, 2013

far offshore. In contrast, most of the NBUS had SST > 20 °C during February 2011 (MSM17/3). In March 2008 (MSM07/2b-3) SST outline an intermediate upwelling intensity in a coastal band of low temperatures. Stronger or weaker upwelling is associated with distinct distributions of the central water masses on the shelf. Mohrholz et al. (2007) found that vigorous cross shelf circulation during phases of strong upwelling suppresses the along-shelf pole-ward undercurrent of SACW from the north. Weak upwelling phases, such as that in February 2011 permit SACW to protrude far southward (Fig. 7d–f). In this situation, this water mass accounted for 70 % of the subsurface water off Walvis Bay (23° S) during weak upwelling. The dominance of SACW was reflected in mid-water O_2 deficits, so that samples with ≥ 80 % SACW were associated with ≤ 50 µmol kg^{-1} O_2 (Fig. 7a–c). During strong and weak upwelling alike and regardless of the SACW contribution, the O_2 concentrations on the shelf off Walvis Bay were < 20 µmol kg^{-1} during all cruises. The contribution of SACW thus sets the precondition for anoxia in bottom waters off Walvis Bay (Monteiro et al., 2008), but O_2 consumption caused by the decomposition of organic matter exported from the surface plays a decisive role (Monteiro et al., 2006; van der Plas et al., 2007).

The N : P deviation from Redfield (as indicated by N*) varied during the different expeditions and upwelling states (Fig. 8). This variability was not apparently tied to the distribution of SACW and O_2 concentrations at offshore sites (Fig. 7a–c). From the temporal variability in patterns of N* in the hemipelagic OMZ offshore of Kunene (17.25° S) it is apparent that N* in the SACW water mass varied significantly between years (Fig. 9). During March 2008 (MSM07/2b-3), N* was 3 fold increased within the OMZ (N* ~ 12 µmol kg^{-1}) compared to December 2009 and February 2011 (N* ~ 3–4 µmol kg^{-1}) indicating that the N* inventory of SACW differs. This positive N* anomaly was imported to the NBUS in 2008 with SACW, so that water masses on the shelf were less N* deficient despite similarly low O_2 concentrations than in 2009 and 2011 (Fig. 8a–c). In contrast to the situation in March 2008 (MSM07/2b-3), most of the NBUS area was N-deficient in December 2009 (Afr258) and February 2011 (MSM17/3) and highest N deficits (N* ~ −35 µmol kg^{-1}) offshore Walvis Bay exceeded the N deficits in

BGD
10, 10459–10489, 2013

March 2008 by a factor of > 2. The results suggest that the considerable variability in nutrient ratios of SACW controls the inter-annual variability of N^* in the NBUS. Positive N^* anomalies in subsurface waters are commonly attributed to the mineralization of organic matter produced by N_2-fixing organisms (Gruber and Sarmiento, 1997) that have N : P ratios of up to 150 (Krauk et al., 2006). Positive N^* anomalies in the tropical and subtropical North Atlantic are $\sim 4\,\mu mol\,kg^{-1}$ at $\sigma_\theta = 26.5$ (Gruber and Sarmiento, 1997; Mahaffey et al., 2005). Here, intensive blooms of *Trichodesmium* spp. (Carpenter, 1983; Tyrrell et al., 2003; Capone et al., 2005) and high N : P (of up to 35) have been reported (Mahaffey et al., 2003) and are consistent with N_2 fixation as a significant input source, which can raise N^* to $\sim 20\,\mu mol\,kg^{-1}$ (Mahaffey et al., 2003). In contrast, the South Atlantic gyre has low positive N^* (Gruber and Sarmiento, 1997), in line with low rates of N_2 fixation (Mahaffey et al., 2005) that has been attributed to a lack of iron (Fe) supply (Moore et al., 2009). However, Sohm et al. (2011) observed N_2 fixation within the ABFZ ($\sim$ 13–15° S) coincident with decreased thermocline $\delta^{15}N^-_{NO_3}$ values and elevated dissolved Fe and cobalt surface concentrations (Noble et al., 2012) that are important micronutrients for marine diazotrophic cyanobacteria (Saito et al., 2002, 2004). The studies of Sohm et al. (2011) and Noble et al. (2012) were performed in November–December 2007 and hence $\sim$ 4 months prior to the MSM07/2b-3 expedition in March 2008 that found the positive N^* anomaly in SACW. Although the N_2 fixation rates measured by Sohm et al. (2011) were relatively low (22–85 µmol N m^{-2} d^{-1}), N_2 fixation north of the ABFZ is the only feasible input source that caused the observed high N excess in the SACW in 2008.

3.3 NBUS – a P*-source for the South Atlantic

Upwelling of N-deficient water in 2009 and 2011 caused lowest N^* at 5 m depth close to the coast (Fig. 8d–f) indicating that a relative P surplus surfaces and is advected offshore into the open ocean with modified upwelling water. This should stimulate N_2 fixation in the adjacent hemipelagic ocean (Deutsch et al., 2007), but experimentally

BGD
10, 10459–10489, 2013

determined rates of N_2 fixation in the NBUS and its periphery were very low to not detectable (N. Wasmund, personal communication, 2012). We calculated the P excess (P^*) within the euphotic zone (0–20 m) that is exported offshore for the Walvis Bay (23° S) transect (Fig. 10). Roughly 300 km offshore, beyond the continental slope, P^* was close to zero in March 2008 ($P^* = 0.007 \pm 0.09\,\mu mol\,kg^{-1}$), suggesting that the NBUS at that time was not a regional P source for the oligotrophic subtropical South Atlantic. During the other cruises, the NBUS was a relative P source with P^* values of $0.3 \pm 0.01\,\mu mol\,kg^{-1}$. These observations are in line with Staal et al. (2007) and Moore et al. (2009) who reported surface $P^* = 0.15$–$0.30\,\mu mol\,kg^{-1}$ within areas of the Subtropical Gyre that are influenced by the advection of water masses transported by the Benguela Current. Along with our findings, it implies that the coastal upwelling system over the shelf is a P^* source to the South Atlantic most of the time. Since the mud belt is a geological feature and the O_2 concentration off Walvis Bay was $< 20\,\mu mol\,kg^{-1}$ independently from the upwelling situation (Fig. 7a–c) it is assumed that the inter-annual variability of that P source depends mainly on the N excess in the SACW that is produced probably by N_2 fixation north of the ABFZ. We further presume that N_2 fixation in this region is in turn linked to the NBUS by the export of P^* into the South Atlantic ocean and its advection along with the major surface currents to the Angola Gyre and ABFZ region (Fig. 11).

4 Conclusions

Our data measured during the cruise in March 2011 show a mean C : N : P : O_2 ratio that is close to the Redfield stoichiometry. Over the mud belt on the Namibian shelf pore water fluxes lowered the C : N : P : O_2 ratio to 106 : 16 : 1.6 : 138. Only in restricted regions were O_2 concentration dropped below $20\,\mu mol\,kg^{-1}$, N losses further increased the C : N and reduced N : P ratios. Additional nutrient data measured during 2 cruises in 2008 and 2009 reveal an inter-annual variability of N excess within the SACW that flows from the north into the NBUS with highest N^* values observed in 2008. The degree to

BGD
10, 10459–10489, 2013

which the N loss on the shelf is balanced by enhanced N inputs along with the SACW controls the amount of P^* that is exported from the NBUS into the subtropical South Atlantic. To better understand the NBUS' role in the coupled C : N : P cycles and its response to global change, factors controlling e.g. the occurrence of N_2 fixation at the ABFZ need to be addressed in future studies.

Acknowledgements. We would like to thank all scientists, technicians, officers and their crews of the research vessels FS *Maria S. Merian* and FRS *Africana*. Particularly, we would like to thank T. Heene and V. Mohrholz from the Leibniz Institute for Baltic Sea Research, Warnemünde for operating the CTD and providing the data. Suzie Christof, N. Moroff and S. Oesterle from the NatMIRC Institute, Swakopmund are thanked for their comprehensive support during the stay in Swakopmund. Matthias Birkicht is acknowledged for the nutrient analysis. We sincerely thank L. Lehnhoff and C. Steigüber for their help during and subsequently to the expeditions. Furthermore, we are grateful to the German Federal Ministry of Education and Research (BMBF, Bonn) for financial support of the GENUS program (03F0497D – ZMT).

References

Anderson, L. A. and Sarmiento, J. L.: Redfield ratios of remineralization determined by nutrient data analysis, Global Biogeochem. Cy., 8, 65–80, 1994.

Arrigo, K. R.: Marine microorganisms and global nutrient cycles, Nature, 437, 349–355, doi:10.1038/nature04158, 2005.

Bailey, G. W. and Chapman, P.: Short-term variability during an anchor study in the southern Benguela upwelling system: chemical and physical oceanography, Prog. Oceanogr., 28, 9–37, 1991.

Behrenfeld, M. J., O'Malley, R. T., Siegel, D. A., McClain, C. R., Sarmiento, J. L., Feldman, G. C., Milligan, A. J., Falkowski, P. G., Letelier, R. M., and Boss, E. S.: Climate-driven trends in contemporary ocean productivity, Nature, 444, 752–755, doi:10.1038/nature05317, 2006a.

Behrenfeld, M. J., Worthington, K., Sherrell, R., Chavez, F. P., Strutton, P., McPhaden, M., and Shea, M. D.: Controls on tropical Pacific Ocean productivity revealed trough nutrient stress analysis, Nature, 442, 1025–1028, doi:10.1038/nature05083, 2006b.

BGD
10, 10459–10489, 2013

Boehme, S. E., Sabine, C. L., and Reimers, C. E.: CO fluxes from a coastal transect: a time-series approach, Mar. Chem., 63, 49–67, 1998.
Bremner, J. M.: Concretionary phosphorite from SW Africa, Geol. Soc., 137, 773–786, 1980.
Bremner, J. M. and Willis, J. P.: Mineralogy and geochemistry of the clay fraction of sediments from the Namibian continental margin and the adjacent hinterland, Mar. Geol., 115, 85–116, 1993.
Broecker, W. S. and Peng, T. H.: Tracers in the Sea, 1982.
Capone, D. G., Burns, J. A., Montoya, J. P., Subramaniam, A., Mahafffey, C., Gunderson, T., Michaels, A. F., and Carpenter, E. J.: Nitrogen fixation by *Trichodesmium* spp.: an important source of new nitrogen to the tropical and subtropical North Atlantic Ocean, Global Biogeochem. Cy., 19, 1–17, 2005.
Carpenter, E. J.: Nitrogen fixation by marine Oscillatoria (Trichodesmium) in the world's oceans, in: Nitrogen in the Marine Environment, edited by: Carpenter, E. J., and Capone, D. G., Academic Press, New York, 65–103, 1983.
Carr, M.-E.: Estimation of potential productivity in Eastern Boundary Currents using remote sensing, Deep-Sea Res. Pt. II, 49, 59–80, 2002.
Deutsch, C., Sarmiento, J. L., Sigman, D. M., Gruber, N., and Dunne, J. P.: Spatial coupling of nitrogen inputs and losses in the ocean, Nature, 445, 163–167, doi:10.1038/nature05392, 2007.
Duncombe Rae, C. M.: A demonstration of the hydrographic partition of the Benguela upwelling ecosystem at 26°40′ S, Afr. J. Mar. Sci., 27, 617–628, 2005.
Emeis, K.-C., Brüchert, V., Curriec, B., Endler, R., Ferdelman, T., Kiessling, A., Leipe, T., Noli-Peard, K., Struck, U., and Vogt, T.: Shallow gas in shelf sediments of the Namibian coastal upwelling ecosystem, Cont. Shelf Res., 24, 627–642, 2004.
Falkowski, P. G.: Evolution of the nitrogen cycle and its influence on the biological sequestration of CO_2 in the ocean, Nature, 387, 272–275, 1997.
Föllmi, K. B.: The phosphorus cycle, phosphogenesis and marine phosphate-rich deposits, Earth-Sci. Rev., 40, 55–124, 1996.
Glenn, C. R., Follmi, K. B., and Riggs, S. R.: Phosphorus and phosphorites: Sedimentology and environments of formation, Eclogae Geol. Helv., 87, 747–788, 1994.
Goldhammer, T., Brüchert, V., Ferdelman, T. G., and Zabel, M.: Microbial sequestration of phosphorus in anoxic upwelling sediments, Nat. Geosci., 3, 557–561, doi:10.1038/NGEO913, 2010.

BGD
10, 10459–10489, 2013

Goldhammer, T., Brunner, B., Bernasconi, S. M., Ferdelman, T. G., and Zabel, M.: Phosphate oxygen isotopes: Insights into sedimentary phosphorus cycling from the Benguela upwelling system, Geochim. Cosmochim. Ac., 75, 3741–3756, 2011.
Gordon, A. L.: South Atlantic thermocline ventilation, Deep-Sea Res., 28, 1239–1264, 1981.
Grasshoff, K., Kremling, K., and Ehrhardt, M.: Methods of seawater analysis, 3rd edn., edited by: Grasshoff, K., Kremling, K., and Ehrhardt, M., Verlag Chemie, 419 pp., 1999.
Gruber, N. and Sarmiento, J. L.: Global patterns of marine nitrogen fixation and denitrification, Global Biogeochem. Cy., 11, 235–266, 1997.
Hall, C. and Lutjeharms, J. R. E.: Cyclonic eddies identified in the Cape Basin of the South Atlantic Ocean, J. Marine Syst., 85, 1–10, doi:10.1016/j.jmarsys.2010.10.003, 2011.
Heinze, C., Maier-Reimer, E., and Winn, K.: Glacial pCO_2 reduction by the world ocean: experiments with the Hamburg Carbon Cycle Model, Paleoceanography, 6, 395–430, 1991.
Hutchings, L., Lingen, C. D. v. d., Shannon, L. J., Crawford, R. J. M., Verheye, H. M. S., Bartholomae, C. H., Plas, A. K. v. d., Louw, D., Kreiner, A., Ostrowski, M., Fidel, Q., Barlow, R. G., Lamont, T., Coetzee, J., Shillington, F., Veitch, J., Currie, J. C., and Monteiro, P. M. S.: The Benguela Current: an ecosystem of four components, Prog. Oceanogr., 83, 15–32, 2009.
Inthorn, M. et al.: Compilation of organic carbon distribution and sedimentology in the surface sediments on the continental margin offshore southwestern Africa, doi:10.1594/PANGAEA.351146, 2006, Supplement to: Inthorn, M., Wagner, T., Scheeder, G., and Zabel, M.: Lateral transport controls distribution, quality and burial of organic matter along continental slopes in high-productivity areas, Geology, 34, 205–208, doi:10.1130/G22153.1, 2006
Ito, T., Follows, M. J., and Boyle, E. A.: Is AOU a good measure of respiration in the oceans?, Geophys. Res. Lett., 31, L17305, doi:10.1029/2004GL020900, 2004.
Kalvelage, T., Jensen, M. M., Contreras, S., Revsbech, N. P., Lam, P., Günter, M., LaRoche, J., Lavik, G., and Kuypers, M. M. M.: Oxygen Sensitivity of Anammox and Coupled N-Cycle Processes in Oxygen Minimum Zones, PLoS ONE, 6, e29299, doi:10.1371/journal.pone.0029299, 2011.
Koeve, W. and Kähler, P.: Heterotrophic denitrification vs. autotrophic anammox – quantifying collateral effects on the oceanic carbon cycle, Biogeosciences, 7, 2327–2337, doi:10.5194/bg-7-2327-2010, 2010.

BGD
10, 10459–10489, 2013

Krauk, J. M., Villareal, T. A., Sohm, J. A., Montoya, J. P., and Capone, D. G.: Plasticity of N : P ratios in laboratory and field populations of *Trichodesium* spp., Aquat. Microb. Ecol., 42, 243–253, 2006.

Kuypers, M. M. M., Lavik, G., Woebken, D., Schmid, M., Fuchs, B. M., Amann, R., Jørgensen, B. B., and Jetten, M. S. M.: Massive nitrogen loss from the Benguela upwelling system through anaerobic ammonium oxidation, P. Natl. Acad. Sci. USA, 102, 6478–6483, 2005.

Lam, P. and Kuypers, M. M.: Microbial nitrogen cycling processes in oxygen mimimum zones, Annu. Rev. Mar. Sci., 3, 317–345, doi:10.1146/annurev-marine-120709-142814, 2010.

Mahaffey, C., Williams, R. G., Wolff, G. A., Mahowald, N., Anderson, W., and Woodward, M.: Biogeochemical signatures of nitrogen fixation in the eastern North Atlantic, Geophys. Res. Lett., 30, 1300, doi:10.1029/2002GL016542, 2003.

Mahaffey, C., Michaels, A. F., and Capone, D. G.: The conundrum of marine N_2 fixation, Am. J. Sci., 305, 546–595, 2005.

McElroy, M. B.: Marine biological controls on atmospheric CO_2 and climate, Nature, 302, 328–329, 1983.

Meeuwis, J. M. and Lutjeharms, J. R. E.: Surface thermal characeristics of the Angola–Bengulea Front, S. Afr. J. Marine Sci., 9, 261–279, 1990.

Mohrholz, V., Bartholomae, C. H., v. d. Plas, A. K., and Lass, H. U.: The seasonal variability of the northern Benguela undercurrent and its relation to the oxygen budget on the shelf, Cont. Shelf Res., 28, 424–441, 2007.

Monteiro, P. M. S., v. d. Plas, A., Mohrholz, V., Mabille, E., Pascall, A., and Joubert, W.: Variability of natural hypoxia and methane in a coastal upwelling system: oceanic physics or shelf biology?, Geophys. Res. Lett., 33, L16614, doi:10.1029/2006GL026234, 2006.

Monteiro, P. M. S., Plas, A. K. v. d., Melice, J.-L., and Florenchie, P.: Interannual hypoxia variability in a coastal upwelling system: ocean-shelf exchange, climate and ecosystem-state implications, Deep-Sea Res. Pt. I 55, 435–450, 2008.

Moore, C. M., Mills, M. M., Achterberg, E. P., Geider, R. J., LaRoche, J., Lucas, M. I., McDonagh, E. L., Pan, X., Poulton, A. J., Rijkenberg, M. J. A., Suggett, D. J., Ussher, S. J., and Woodward, E. M.: Large-scale distribution of Atlantic nitrogen fixation controlled by iron availability, Nat. Geosci., 2, 867–871, doi:10.1038/NGEO667, 2009.

Nagel, B., Emeis, K.-C., Flohr, A., Rixen, T., Schlarbaum, T., Mohrholz, V., and v. d. Plas, A.: N-cycling and balancing of the N-deficit generated in the oxygen minimum zone over the

BGD
10, 10459–10489, 2013

Namibian shelf – an isotope-based approach, J. Geophys. Res.-Biogeo., 118, 367–371, doi:10.1002/jgrg.20040, 2013.
Nathan, Y., Bremner, J. M., Loewenthal, E. R., and Monteiro, P.: Role of bacteria in phosphorite genesis, Geomicrobiol. J., 11, 69–76, doi:10.1080/01490459309377935, 1993.
Noble, A. E., Lamborg, C. H., Ohnemus, D. C., Lam, P. J., Goepfert, T. J., Measures, C. I., Frame, C. H., Casciotti, K. L., DiTullio, G. R., Jennings, J., and Saito, M. A.: Basin-scale inputs of cobalt, iron, and manganese from the Benguela–Angola front to the South Atlantic Ocean, Limnol. Oceanogr., 57, 989–1010, doi:10.4319/lo.2012.57.4.0989, 2012.
Poole, R. and Tomczak, M.: Optimum multiparameter analysis of the water mass structure in the Atlantic Ocean thermocline, Deep-Sea Res. Pt. I, 46, 1895–1921, 1999.
Redfield, A. C., Ketchum, B. H., and Richards, F. A.: The influence of organisms on the composition of seawater, in: The Sea, edited by: Hill, M. N. E., Wiley-Interscience, New York, 1963.
Riebesell, U., Schulz, K. G., Bellerby, R. G. J., Botros, M., Fritsche, P., Meyerhöfer, M., Neill, C., Nondal, G., Oschlies, A., Wohlers, J., and Zöllner, E.: Enhanced biological carbon consumption in a high CO_2 ocean, Nature, 450, 545–549, doi:10.1038/nature06267, 2007.
Saito, M. A., Moffet, J. M., Chisholm, S. W., and Waterbury, J. B.: Cobalt limitation and uptake in *Prochlorococcus*, Limnol. Oceanogr., 47, 1629–1636, 2002.
Saito, M. A., Moffet, J. M., and DiTullio, G. R.: Cobalt and Nickel in the Peru upwelling region: a major flux of labile cobalt utilized as a micronutrient, Global Biogeochem. Cy., 18, GB4030, doi:10.1029/2003GB002216, 2004.
Schulz, H. N. and Schulz, H. D.: Large sulfur bacteria and the formation of phosphorite, Science, 307, 416–418, 2005.
Shannon, L. V.: The Benguela Ecosystem: 1. evolution of the Benguela, physical features and processes, Oceanogr. Mar. Biol., 23, 105–182, 1985.
Shillington, F., Reason, C. J. C., Duncombe Rae, C. M., Florenchie, P., and Penven, P.: Large scale physical variability of the Benguela Current Large Marine Ecosystem (BCLME), in: Benguela: Predicting a Large Marine Ecosystem, Large Marine Ecostystems, edited by: Shannon, V., Hempel, G., Malanotte-Rizzoli, P., Moloney, C., and Woods, J., Elsevier, Amsterdam, 2006.
Sohm, J. A., Hilton, J. A., Noble, A. E., Zehr, J. P., Saito, M. A., and Webb, E. A.: Nitrogen fixation in the South Atlantic Gyre and the Benguela Upwelling System, Geophys. Res. Lett., 38, L16608, doi:10.1029/2011GL048315, 2011.

BGD
10, 10459–10489, 2013

Sprintall, J. and Tomczak, M.: On the formation of central water and thermocline ventilation in the Southern Hemisphere, Deep-Sea Res. Pt. I, 40, 827–848, 1993.
Staal, M., te Lintel Hekkert, S., Brummer, G. J., Veldhuis, M., Sikkens, C., Persijn, S., and Stal, L. J.: Nitrogen fixation along a north-south transect in the eastern Atlantic Ocean, Limnol. Oceanogr., 52, 1305–1316, 2007.
Stramma, L. and England, M.: On the water masses and mean circulation of the South Atlantic Ocean, J. Geophys. Res., 104, 20863–20883, doi:10.1029/1999jc900139, 1999.
Takahashi, T., Broecker, W., and Langer, S.: Redfield ratio based on chemical data from isopycnal surfaces, J. Geophys. Res., 90, 6907–6924, 1985.
Torres, R., Turner, D. R., Silva, N., and Rutllant, J.: High short-term variability of CO_2 fluxes during an upwelling event off the Chilean coast at 30° S, Deep-Sea Res. Pt. I, 46, 1161–1179, 1999.
Tyrrell, T. and Lucas, M. I.: Geochemical evidence of denitrification in the Benguela upwelling system, Cont. Shelf Res., 22, 2497–2511, 2002.
Tyrrell, T., Maranon, E., Poulton, A. J., Bowie, A. R., and Harbour, D. S.: Large-scale latitudinal distribution of *Trichodesmium* spp. in the Atlantic Ocean, J. Plankton Res., 25, 405–416, 2003.
van der Plas, A. K., Monteiro, P. M. S., and Pascall, A.: Cross-shelf biogeochemical characteristics of sediments in the central Benguela and their relationship to overlying water column hypoxia, Afr. J. Mar. Sci., 29, 37–47, 2007.
Watson, A. J., Bakker, D. C. E., Ridgwell, A. J., Boyd, P. W., and Law, C. S.: Effect of iron supply on Southern Ocean CO_2 uptake and implications for glacial atmospheric CO_2, Nature, 407, 730–733, 2000.
Weeks, S. J., Currie, B., and Bakun, A.: Massive emissions of toxic gas in the Atlantic, Nature, 415, 493–494, 2002.

BGD
10, 10459–10489, 2013

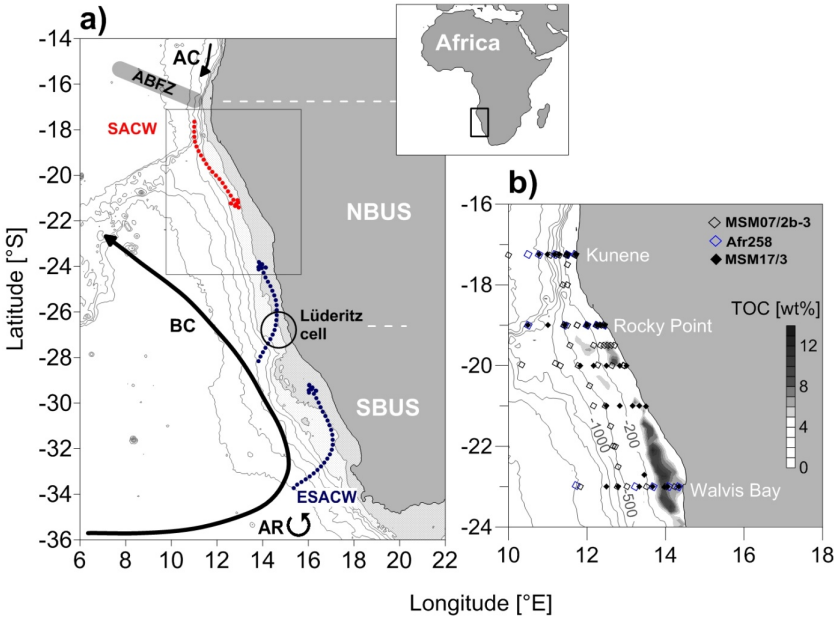

Fig. 1. (a) Schematic overview of the the Benguela upwelling regime located at the south western African coast. Surface currents and features are represented by solid und subsurface currents by dotted lines. AC, Angola Current; ABFZ, Angola–Benguela–Frontal–Zone; AR, Agulhas Rings; BC, Benguela Current; ESACW, Eastern South Atlantic Central Water; NBUS, northern Benguela upwelling system; SACW, South Atlantic Central Water; SBUS, souhern Benguela upwelling system. **(b)** The stations sampled during the cruises: MSM07/2b-3 (open black-edged diamonds), Afr258 (open blue-edged diamonds) and MSM17/3 (black filled diamonds). The grey shading refers to the TOC content (wt. %) of the surface sediments representing the diatomaceous mud belt (TOC data taken from Inthorn et al., 2006).

BGD
10, 10459–10489, 2013

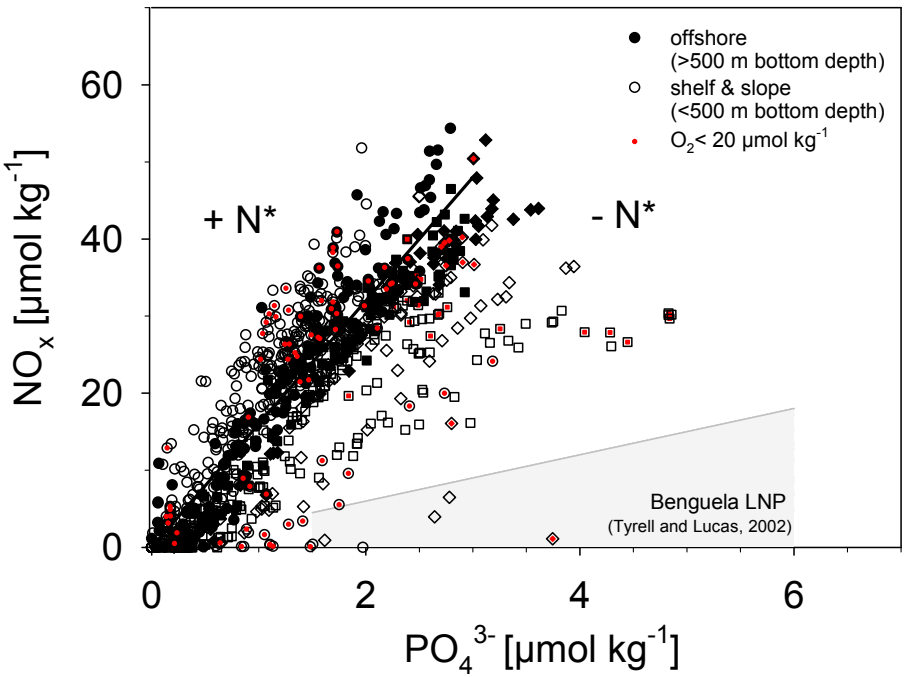

Fig. 2. Composite of NO_x versus PO_4^{3-} ($\mu mol\,kg^{-1}$) data of the MSM07/2b-3 cruise (dots), Afr258 cruise (diamonds) and MSM17/3 cruise (squares). The data was seperated into shelf and slope stations (< 500 m bottom depth) indicated by open symbols and offshore stations (> 500 m bottom depth) indicated by black filled symbols. The red edging corresponds to data points associated to O_2 concentrations ≤ 20 $\mu mol\,kg^{-1}$. Positive and negative deviations from the expected N : P corrleation of 16 : 1 (black line) are expressed in $+N^*$ and $-N^*$ (Gruber and Sarmiento, 1997). The grey shaded area refers to the range of low nitrate:phosphate (LNP) defined by Tyrell and Lucas (2002).

BGD
10, 10459–10489, 2013

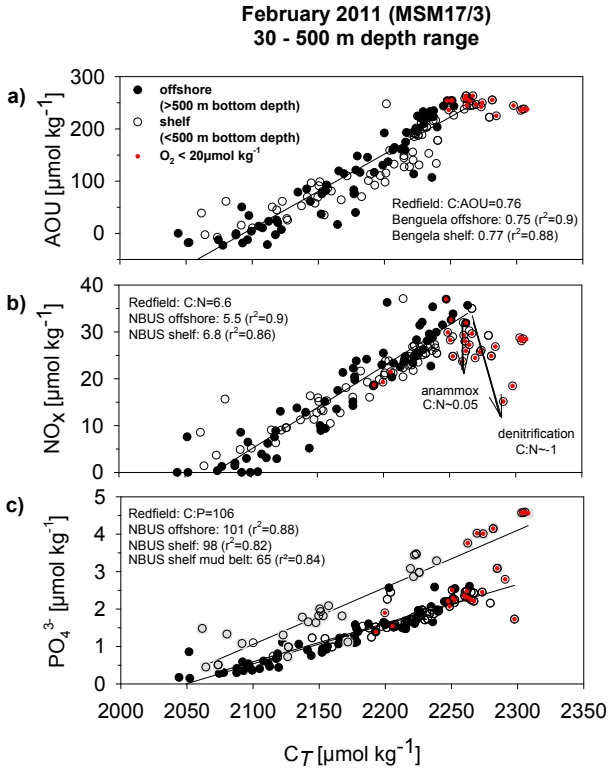

Fig. 3. (a) AOU, **(b)** NO_x and **(c)** PO_4^3 versus C_T (all in µmol kg^{-1}) as measured during the MSM17/3 cruise in February 2011 within the range of 30–500 m water depth. Black filled dots indicate offshore stations and open circles represent slope and shelf stations. Data points associated to O_2 concentrations ≤ 20 µmol kg^{-1} are represented by red filling. The correlations observed for the Benguela are given and indicated by the black line. The reported ratios in panel **(a)** and **(b)** are derived by excluding the ≤ 20 µmol kg^{-1} data. The grey squares in panel **(c)** represent data from the mud belt region.

BGD
10, 10459–10489, 2013

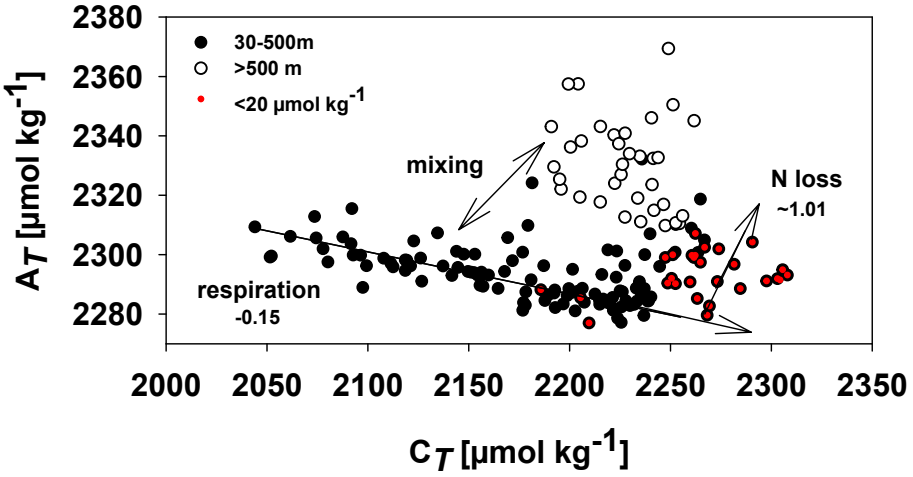

Fig. 4. Salinity corrected total alkalinity (A_T) versus the dissolved inorganic carbon (C_T) (both in µmol kg^{-1}) as measured in February 2011 (MSM17/3) from 30 m depth. Samples associated to the depth range of 30–500 m depth are indicated by black filled circles, samples associated to > 500 m depth are indicated by white filling, samples related to $O_2 < 20$ µmol kg^{-1} are marked by red filling. The solid black lines indicates the expected corrleation caused by aerobic mineralization $A_T : C_T = -16 : 106 = -0.15$ (Redfield et al.,1963) and N consumption, e.g. du to denitrification $A_T : C_T = 104 : 106 = 1.01$ (Gruber and Sarmiento, 1997).

BGD
10, 10459–10489, 2013

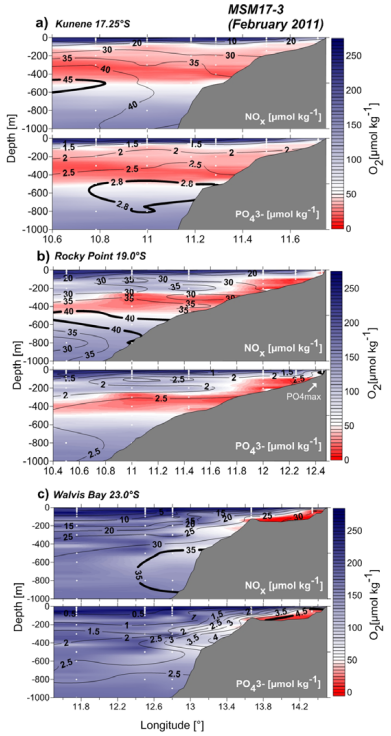

Fig. 5. Vertical section of **(a)** 17.25, **(b)** 19.0 and **(c)** 23.0° S transects during MSM17/3. The O_2 concentration is represented by colour shading and overlain by the NO_x and PO_4^{3-} concentrations (all in µmol kg^{-1}) indicated by the black isolines. The maximum concentrations are represented by a bold black line. The sampled stations used for gridding are marked by white dots.

BGD
10, 10459–10489, 2013

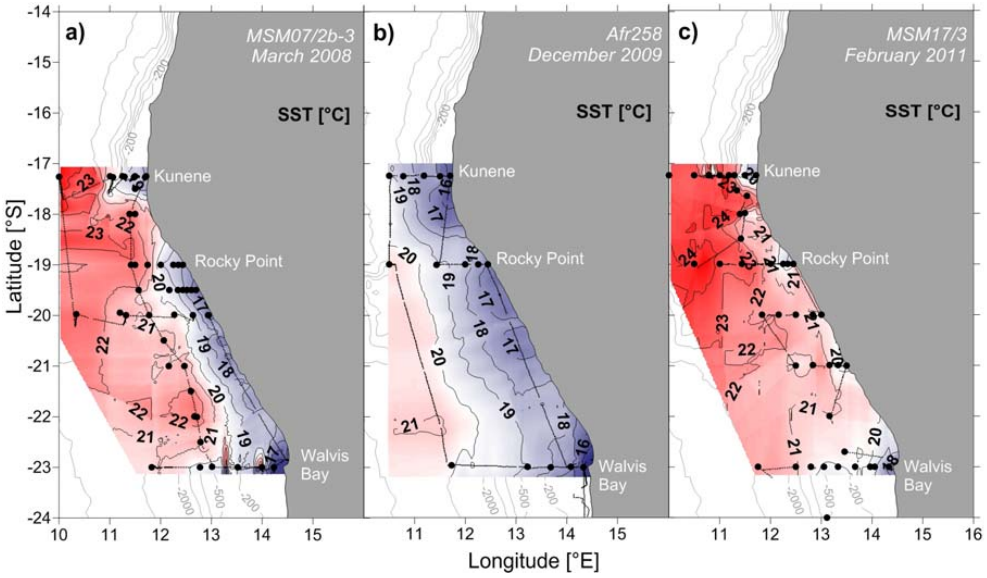

Fig. 6. Distribution of sea surface temperature (SST) (contoured at 1 °C intervals) as measured at 5 m depth continuously along the cruise track during cruise **(a)** MSM07/2b-3, **(b)** Afr258 and **(c)** MSM17/3. The gridding was performed on the basis of data points represented by the black line (cruise track) and black dots (sampled stations).

BGD
10, 10459–10489, 2013

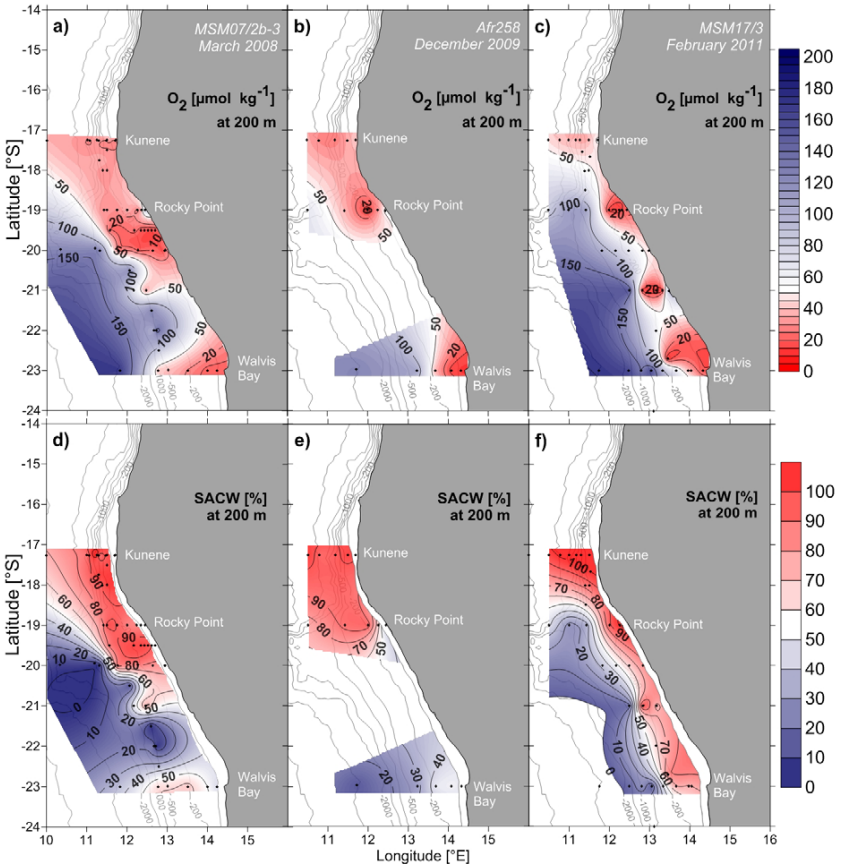

Fig. 7. (a–c) Distribution of O_2 (µmol kg^{-1}) and **(d–f)** SACW portion (%) at 200 m depth. Note: the shelf stations with bottom depths < 200 m were included in the O_2 interpolation and > 100 m in the SACW interpolation. The sampled stations used for gridding are marked by black dots. 0 % SACW is equal to 100 % ESACW.

BGD
10, 10459–10489, 2013

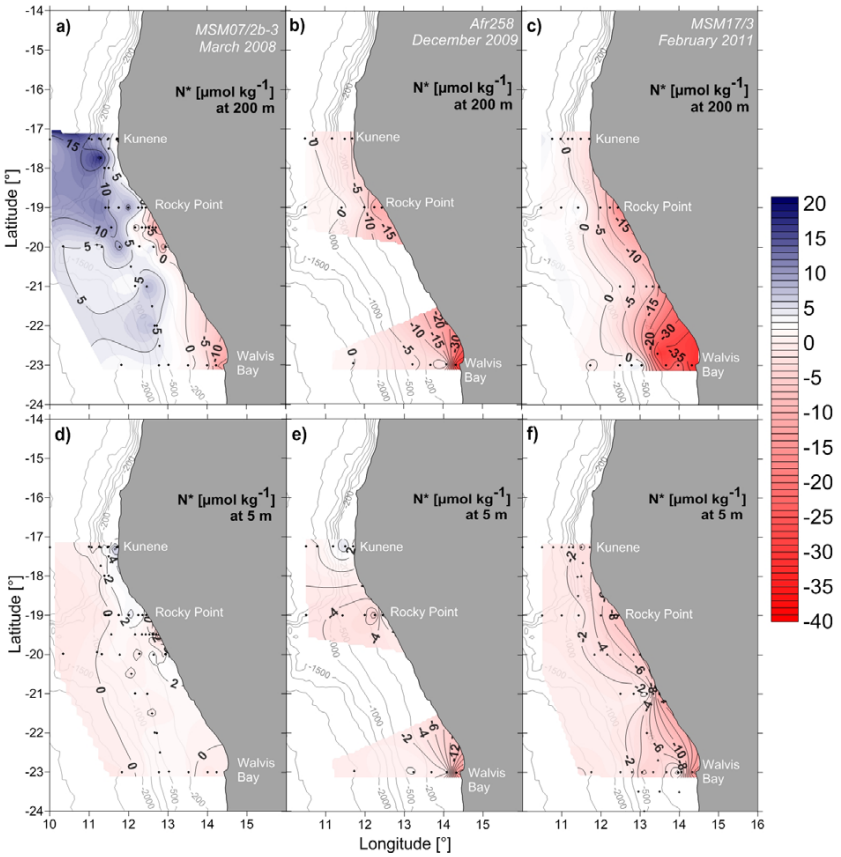

Fig. 8. Distribution of N* (µmol kg^{-1}) **(a–c)** at 200 m and **(d–e)** at 5 m water depth represented by colour shading and isolines. Note: the shelf stations with bottom depths < 200 m were included in the N* interpolation. The sampled stations used for gridding are marked by black dots.

BGD
10, 10459–10489, 2013

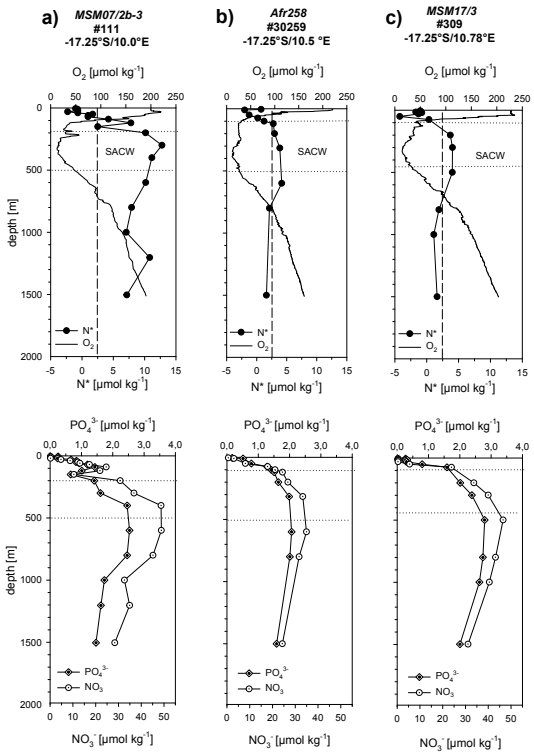

Fig. 9. Vertical profiles of N^*, O_2, NO_3^- and PO_4^{3-} (all in µmol kg^{-1}) as measured during **(a)** MSM07/2b-3, **(b)** Afr258 and **(c)** MSM17/3 at offshore stations with comparable location along the Kunene (17.25° S) transect. The horizontal, dotted lines represent the depth range where high fractions of SACW were detected (90–100 %). The reference value of $N^* = 2.5$ µmol kg^{-1} that results from the N^* equation given by Gruber and Sarmiento (1997) is indicated by the vertical dashed line.

BGD
10, 10459–10489, 2013

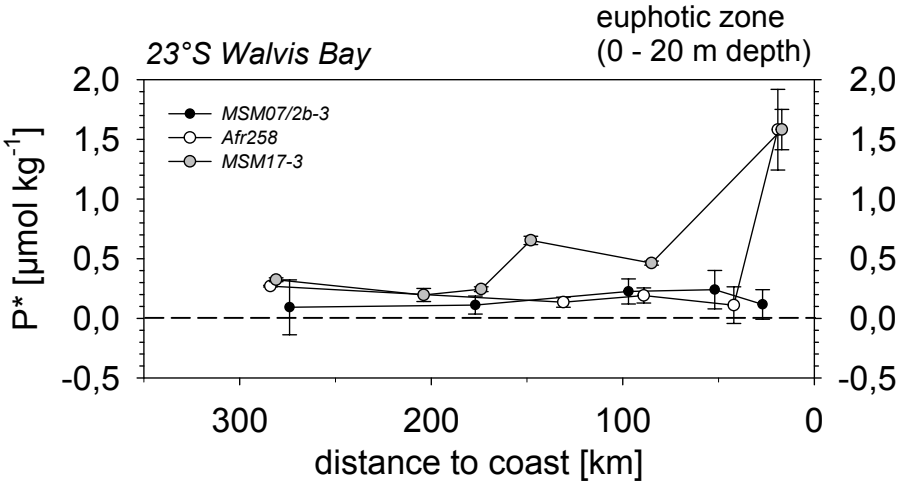

Fig. 10. Averaged P* (µmol kg^{-1}) within the euphotic zone (0–20 m water depth) versus distance to the coast (km) as observed during MSM07/2b-3 (black filled circle), Afr258 (open circle) and MSM17/3 (grey filled circle).

BGD
10, 10459–10489, 2013

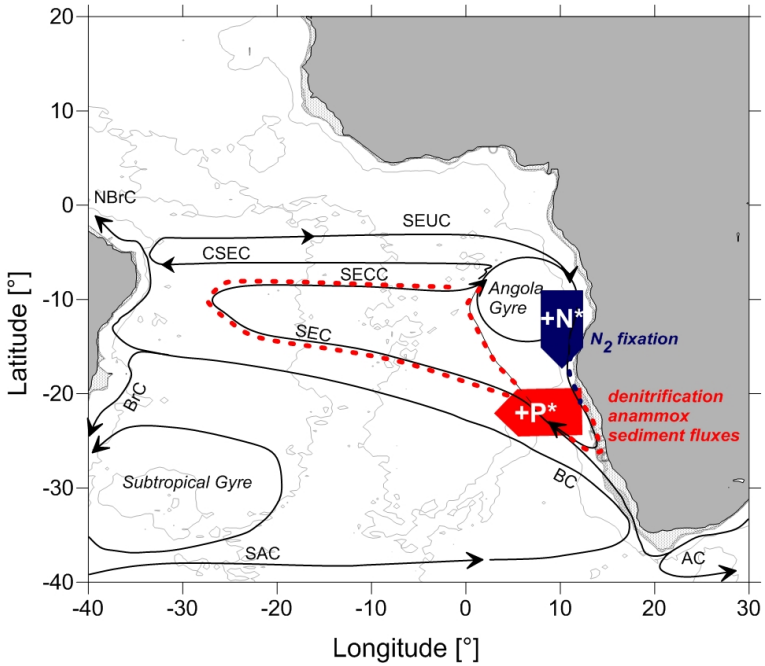

Fig. 11. Map of the wind driven large scale circulation (100–500 m depth range) of the South Atlantic Ocean (adapted from Stramma and England, 1999). The map illustrates the hypothetical advection of the $+P^*$ (red dashed line) via SEC and SECC towards the Angola Gyre where it fuels N_2 fixation and in turn results in a relative N excess ($+N^*$, blue dashed line) that is introduced to the NBUS. The −200 m and −500 m isobaths are represented by grey shading. AC, Agulhas Current; BC, Benguela Current; BrC, Brazil Current; CSEC, Central South Equatorial Current; NBrC; North Brazil Current; SAC, South Atlantic Current; SEC, South Equatorial Current; SECC, South Equatorial Countercurrent; SEUC, South Equatorial Undercurrent.

BGD
10, 10459–10489, 2013